Elsevier Editorial System(tm) for Gastrointestinal Endoscopy
Manuscript Draft

Manuscript Number: GIE-D-11-00936R1

Title: Vital-dye enhanced fluorescence imaging of gastrointestinal mucosa: metaplasia, neoplasia, inflammation

Article Type: New Methods & Materials

Keywords: fluorescence imaging, Barrett's esophagus, esophageal adenocarcinoma, colonic adenocarcinoma, inflammatory bowel disease

Corresponding Author: Ms. Nadhi Thekkek, B.S.

Corresponding Author's Institution: Rice University

First Author: Nadhi Thekkek, B.S.

Order of Authors: Nadhi Thekkek, B.S.; Timothy J Muldoon, M.D., Ph.D.; Alexandros D Polydorides, M.D., Ph.D.; Dipen M Maru, M.D.; Noam Harpaz, M.D., Ph.D.; Michael T Harris, M.D.; Wayne Hofstettor, M.D.; Spiros P Hiotis, M.D.; Sanghyun A Kim, M.D.; Alex J Ky, M.D.; Sharmila Anandasabapathy, M.D.; Rebecca Richards-Kortum, Ph.D.

Manuscript Region of Origin: US Multicenter

Abstract: Abstract
Background: Confocal endomicroscopy has revolutionized endoscopy by offering sub-cellular images of gastrointestinal epithelium; however, field-of-view is limited. There is a need for multi-scale endoscopy platforms that use widefield imaging to better direct placement of high-resolution probes.

Design: Feasibility Study

Objective: This study evaluates the feasibility of a single agent, proflavine hemisulfate, as a contrast medium during both widefield and high resolution imaging to characterize morphologic changes associated with a variety of gastrointestinal conditions.

Setting: U.T. M.D. Anderson Cancer Center (Houston, TX) and Mount Sinai Medical Center (New York, NY)

Patients, Interventions, and Main Outcome Measurements: Surgical specimens were obtained from 15 patients undergoing esophagectomy/colectomy. Proflavine, a vital fluorescent dye, was applied topically. Specimens were imaged with a widefield multispectral microscope and a high-resolution microendoscope. Images were compared to histopathology.

Results: Widefield-fluorescence imaging enhanced visualization of morphology, including the presence and spatial distribution of glands, glandular distortion, atrophy and crowding. High-resolution imaging of widefield-abnormal areas revealed that neoplastic progression corresponded to glandular heterogeneity and nuclear crowding in dysplasia, with glandular effacement in carcinoma. These widefield and high-resolution image features correlated well with histopathology.
Limitations: This imaging approach must be validated in vivo with a larger sample size.

Conclusions: Multi-scale proflavine-enhanced fluorescence imaging can delineate epithelial changes in a variety of gastrointestinal conditions. Distorted glandular features seen with widefield imaging could serve as a critical 'bridge' to high-resolution probe placement. An endoscopic platform combining the two modalities with a single vital-dye may facilitate point-of-care decision-making by providing real-time, in vivo diagnoses.

Abstract

Background: Confocal endomicroscopy has revolutionized endoscopy by offering sub-cellular images of gastrointestinal epithelium; however, field-of-view is limited. There is a need for multi-scale endoscopy platforms that use widefield imaging to better direct placement of high-resolution probes.

Design: Feasibility Study

Objective: This study evaluates the feasibility of a single agent, proflavine hemisulfate, as a contrast medium during both widefield and high resolution imaging to characterize morphologic changes associated with a variety of gastrointestinal conditions.

Setting: U.T. M.D. Anderson Cancer Center (Houston, TX) and Mount Sinai Medical Center (New York, NY)

Patients, Interventions, and Main Outcome Measurements: Surgical specimens were obtained from 15 patients undergoing esophagectomy/colectomy. Proflavine, a vital fluorescent dye, was applied topically. Specimens were imaged with a widefield multispectral microscope and a high-resolution microendoscope. Images were compared to histopathology.

Results: Widefield-fluorescence imaging enhanced visualization of morphology, including the presence and spatial distribution of glands, glandular distortion, atrophy and crowding. High-resolution imaging of widefield-abnormal areas revealed that neoplastic progression corresponded to glandular heterogeneity and nuclear crowding in

dysplasia, with glandular effacement in carcinoma. These widefield and high-resolution image features correlated well with histopathology.

Limitations: This imaging approach must be validated *in vivo* with a larger sample size.

Conclusions: Multi-scale proflavine-enhanced fluorescence imaging can delineate epithelial changes in a variety of gastrointestinal conditions. Distorted glandular features seen with widefield imaging could serve as a critical 'bridge' to high-resolution probe placement. An endoscopic platform combining the two modalities with a single vital-dye may facilitate point-of-care decision-making by providing real-time, *in vivo* diagnoses.

Background

In the surveillance of both Barrett's esophagus (BE) and Inflammatory Bowel Disease (IBD), dysplasia is often focal, flat and indistinguishable from non-dysplastic mucosa[1, 2]. Current white-light endoscopic platforms lack the resolution required to accurately identify dysplasia. As a result, over half of such lesions can be missed[2-4].

Confocal endomicroscopy has revolutionized endoscopy by offering sub-cellular images of gastrointestinal epithelium[5-7]. However, the increase in spatial resolution comes at the expense of decreased field of view, leaving large areas unsurveyed. Therefore, there exists a need for multi-scale endoscopy platforms that use widefield imaging to better direct placement of high-resolution fluorescent imaging devices, including the recently described high-resolution microendoscope, an inexpensive (<$5000), probe-based technology for imaging histologic features in vivo[8, 9].

Our goal in this *ex vivo* feasibility study was to evaluate the feasibility of a single topical contrast agent (0.01% proflavine hemisulfate) using a prototype multi-scale, fluorescence-based platform using both widefield and high-resolution imaging of the esophagus and colon using a single topical contrast agent (0.01% proflavine hemisulfate). Resulting images were compared to standard H&E-stained histopathology to determine what morphologic features associated with metaplasia, neoplasia, and inflammation can be visualized using this novel approach. These criteria may be used in future *in vivo* studies to determine its impact on diagnostic accuracy and margin determination.

Methods

Specimen Preparation and Imaging

Patients at UT MD Anderson Cancer Center and Mount Sinai Medical Center undergoing endoscopic mucosal resection (EMR) or surgery for adenocarcinoma or intractable IBD gave written informed consent to participate.

Immediately following resection, the mucosal surface of each specimen was rinsed with saline and imaged under white light illumination. Abnormal and normal areas were identified by the study pathologist based on appearance; borders of these regions were marked on the white light image. Proflavine hemisulfate (0.01% w/v), which has been shown to localize in cell nuclei[8, 10], was applied to the mucosal surface for 30 seconds. Excess proflavine was removed with dry gauze.

Widefield fluorescence images of areas identified as grossly normal and abnormal were obtained using a multispectral digital microscope (MDM)[11]. High-resolution fluorescence images were subsequently obtained from areas imaged with the MDM using a high resolution microendoscope (HRME)[8, 12]. In an effort to reduce sampling error, a dot of India ink was placed at each area imaged with the HRME, fixed with acetic acid, and photographed. Since the ink spread to ~2-4 mm in diameter and the field of view of the HRME is 750 µm, the photograph guided the approximation of image sites on large resected specimens; necessary to facilitate registration between widefield imaging, high resolution imaging, and subsequent histopathologic evaluation.

The specimen was then fixed in formalin and submitted for standard histopathologic analysis; vertical cross-sections were examined to grade and verify presence of disease. The study pathologist, blinded to the image results, assigned diagnoses to histologic sections of inked areas using standard histologic criteria.

Instrumentation

The MDM, a surgical microscope modified for fluorescence imaging, has been described previously[11]. In this study, widefield images were obtained at 450 nm excitation, and fluorescence was collected through a 515 nm long-pass filter. The field of view of the MDM is 2.5 cm, with a spatial resolution of 50-100 um. The average

illumination intensity was 2.14 mW/cm^2 and images were acquired with a 1 s integration time.

The HRME system has also been described[8]. Illumination was provided via a 450 nm LED coupled to a coherent fiber-optic bundle. Fluorescence collected by the bundle while in contact with the tissue was delivered to a CCD camera through a 490 nm long pass filter. The field of view of the HRME is 750 μm in diameter and the spatial resolution is 4.5 microns.

Image Assessment

Fluorescence images were qualitatively compared to histology images. Features evaluated in widefield images included the presence or absence of glandular epithelium in the esophagus (Barrett's metaplasia), and the architectural characteristics of the colonic epithelium (shape, size, and spatial distribution of crypts, presence/absence of glandular distortion). Features evaluated in high-resolution images included nuclear size, density, orientation and homogeneity as well as the composition of the lamina propria.

Results

Resected specimens from 15 patients were evaluated, including; 9 EMRs and 2 esophagectomies from patients with Barrett's-associated neoplasia, 3 colectomies from patients with colorectal adenocarcinoma, and 3 colectomies from patients with IBD (2 with ulcerative colitis and 1 with Crohn's disease). Images were obtained from 36 individual histologically-verified sites. Each figure shows a white light image, a widefield proflavine-fluorescence image, corresponding high resolution fluorescence image, and pathology. The inked area is approximated by a circle in each of the widefield proflavine-fluorescence images.

Figure 1 shows images of esophageal mucosa. The top region of the white light image (Figure 1A) depicts an area of normal esophageal squamous mucosa. The corresponding area in the widefield proflavine-fluorescence image (Figure 1B) shows homogeneous fluorescence, with uniform intensity except for some apparent proflavine pooling in tissue folds (arrow). A representative high-resolution image of the squamous region (Figure 1C) exhibits hexagonally-shaped cells with bright, small, round, evenly-spaced nuclei, which were consistently observed. These features are apparent in the corresponding histology section of the epithelial surface (Figure 1D).

During white light imaging, the glandular architecture of BE is difficult to visualize. In contrast, during widefield proflavine-fluorescence imaging, the glandular architecture is easily appreciated (Figure 1B). A high-resolution image (Figure 1E) obtained from the circled area shows glands with central dark lumens, lined by evenly spaced cells with small, regular and polarized nuclei. Similar features are seen in histologic sections from the corresponding area (Figure 1F), which include metaplastic columnar epithelium with intestinal-type goblet cells.

Figure 2 shows images of Barrett's-associated neoplastic changes. Figure 2A shows a standard, white-light image of an area of BE with high grade dysplasia (HGD) and adenocarcinoma. In the corresponding widefield proflavine-fluorescence image (Figure 2B), glands appear irregular compared to the glands associated with BE. Note the visible India ink (arrow). The high-resolution image (Figure 2C) obtained from the circled area shows glands that are smaller, more irregular in shape and irregularly spaced, compared to the glands in non-neoplastic BE. In addition, nuclei are more numerous, crowded, pleomorphic, and have lost polarity (arrow), mirroring the appearance of HGD and adenocarcinoma seen in the corresponding histologic section (Figure 2D).

Figure 3 shows images of normal colonic mucosa. Figure 3A depicts normal colonic mucosa under white light illumination. The glandular pattern of colonic mucosa is more apparent with widefield proflavine-fluorescence imaging (Figure 3B). The corresponding high-resolution image (Figure 3C) from the circled region is characterized by evenly distributed, round tubular structures of similar shape and diameter (yellow arrow) with basally oriented, small, fluorescent nuclei (white arrow), features that correlate well with the transverse histologic section from the same area (Figure 3D).

Figure 4 shows images from the edge of colonic dysplasia. Under white light (Figure 4A) colonic ridges are visualized as well as the transition to an area of irregular growth. With proflavine-enhanced widefield imaging (Figure 4B), dysplastic glandular structures appear larger than normal colonic crypts and are not as evenly spaced. In the corresponding high-resolution fluorescence imaging (Figure 4C) of the circled area, glands appear elongated and irregular (yellow arrow) with apparent nuclear crowding (white arrow). These features correspond to the dysplastic colonic mucosa in the histologic section (Figure 4D).

Figure 5 shows images of severe dysplasia. Under white light (Figure 5A), the surface of a lesion can be appreciated, but without much glandular detail. In the corresponding widefield proflavine-fluorescence image (Figure 5B), barely-visible glands appear distorted. High-resolution imaging (Figure 5C) of the region indicated by the circle reveals irregular and unevenly spaced glandular structures (yellow arrow) composed of crowded cells with enlarged, fluorescent nuclei that are heterogeneously oriented (white arrow), features that correspond to the diagnosis of HGD seen in the corresponding histologic section (Figure 5D).

Figure 6 shows images from an area of invasive adenocarcinoma. A mass is visible under white light (Figure 6A) and poorly-formed glandular structures can be seen during widefield proflavine-fluorescence imaging (Figure 6B). The high-resolution image

(Figure 6C) of the circled area reveals highly irregular and uneven tubular structures lined by enlarged, fluorescent nuclei lacking orientation and polarity. The intervening stroma appears crowded, contributing to the visible increase in fluorescence. These features mirror the appearance of dysplastic glands amidst desmoplastic stromal reaction in the corresponding histologic section (Figure 6D), which are diagnostic of invasive colorectal adenocarcinoma.

Figure 7 shows images depicting mildly-active IBD. In the white-light image (Figure 7A) glandular detail is not easily appreciated. However, in the fluorescence images (Figure 7B-C), glands appear distorted and slightly more irregular in spacing than in normal colonic mucosa and in quiescent IBD (not shown). The increase in glandular distortion, cryptitis (arrow), and the expanded lamina propria seen in the high-resolution image are consistent with the abnormalities seen in the corresponding histologic section showing active colitis (Figure 7D). This patient was known to have ulcerative colitis clinically.

Figure 8 shows an example of severely-active IBD. In the white-light image (Figure 8A), the presence of inflammation and ulceration make glands difficult to visualize. In the widefield proflavine-fluorescence image (Figure 8B) the glands appear irregular and disorganized. The high-resolution image obtained from the circled region (Figure 8C) shows a dense population of fluorescent inflammatory cells. These features correspond to the ulcer bed seen in the corresponding histologic section showing severe colitis (Figure 8D), with chronic inflammatory cells in the lamina propria and extensive gland dropout. This patient was known to have active Crohn's disease clinically.

Tables 1-3 summarize the morphologic features consistently observed in widefield and high-resolution imaging in Barrett's-associated neoplasia, colonic neoplasia, and IBD. Following application of proflavine, widefield fluorescence images consistently identify larger-scale architectural differences in glandular size, shape, and

distribution, while high-resolution images consistently allows assessment of nuclear crowding.

Discussion

This ex vivo pilot study demonstrates the technical feasibility of a new multi-scale imaging approach, in which sequential widefield and high-resolution fluorescence imaging is performed using a single fluorescent vital dye. Results indicate that multi-scale, proflavine-enhanced, fluorescence imaging can characterize glandular and cellular changes associated with metaplasia, neoplasia, and inflammation in gastrointestinal (GI) mucosa. Features visible with both modalities correlate well with those observed during standard histopathologic evaluation.

The results of this study provide a rationale to evaluate this multi-scale surveillance technique in vivo; further studies are necessary to determine whether similar conclusions can be drawn during endoscopic imaging of proflavine. Moreover, larger sample sizes are required to assess the sensitivity and specificity of this approach. Despite these limitations, this study suggests that multi-scale fluorescence imaging has the potential to address some of the limitations of existing widefield and high-resolution endoscopic platforms.

Existing widefield endoscopic imaging techniques are emerging as promising ways to improve early detection of precancerous lesions by scanning over a large surface area. For example, autofluorescence imaging detects changes in stromal fluorescence with high sensitivity; however, it is limited by low specificity[4, 13, 14]. Narrowband imaging detects differences in vascular density, however it only indirectly visualizes glandular architecture. In the imaging platform described here, widefield

fluorescence imaging is used to provide direct visualization of glandular morphology, providing valuable information on alterations that are visible in H&E-stained tissue sections.

The relatively poor specificity of widefield imaging motivates the need for high-resolution interrogation at the cellular level. Confocal imaging, using IV fluorescein to enhance imaging of vasculature, is the most accurate high-resolution imaging technique to date[5, 6]. Though its use in vivo is well established, cost may prevent it from being used outside tertiary care centers. Its published accuracy requires IV administration of fluorescein, further complicating the potential for widespread use. High-resolution imaging with topical proflavine can achieve sub-cellular resolution with less expensive instrumentation[8]. Topical proflavine stains nuclei, allowing direct visualization of relevant histologic features (e.g., nuclear density) associated with neoplasia. Though other promising technologies such as endocytoscopy, a probe-based technology used in conjunction with methylene blue, also allow direct visualization of histologic features[15, 16], by using the HRME with a fluorescent dye, imaging can be accomplished without having the dye interfere with standard white light imaging.

Using proflavine as a contrast agent for both widefield and high-resolution techniques provides an advantage over existing platforms which require different contrast agents for sequential imaging (e.q., methylene blue chromoendoscopy followed by confocal microendoscopy with fluorescein)[17]. Proflavine is a component of acriflavine, which has been used in vivo in GI imaging studies[18]. It is a major component of triple dye, which is widely used as an antiseptic regimen in the care of newborn umbilical cords[19]; our study concentration is ten times less than the concentration in triple dye. These precedents, coupled with promising initial results support future in vivo use of proflavine for multi-scale imaging of GI mucosa.

Widefield fluorescence imaging of proflavine would enhance the ability of gastroenterologists to examine glandular architecture over large areas of the GI mucosa. Suspicious areas would then be interrogated further with high-resolution imaging using the same contrast agent to reveal sub-cellular changes associated with nuclear morphology. This multi-scale approach may increase sampling efficiency, enhance dysplasia detection and improve margin determination.

Acknowledgement: The authors acknowledge Rachna Muldoon for her invaluable assistance during this study. This work is supported through the National Institute of Health grants BRP CA103830, RO1 EB007594 and 1R01CA140257-01A1.

Figure Captions:

Figure 1: White-light image of squamo-columnar junction is shown (A). Widefield proflavine-fluorescence image (B) shows glandular detail in the Barrett's region. High-resolution fluorescence image of squamous mucosa is shown (C) with corresponding histopathology (D). High-resolution image of BE from area, indicated in (B), shows large glands typical of intestinal metaplasia (E). Corresponding histopathology is shown in (F).

Figure 2: White-light image of Barrett's-associated neoplasia is shown (A). Widefield proflavine-fluorescence image depicts irregular glands (B). High-resolution fluorescence image from area indicated in (B) shows areas of nuclear crowding (arrow) (C). Corresponding histopathology is shown (D).

Figure 3: White-light image normal colonic mucosa is shown (A). Widefield proflavine-fluorescence image shows evenly-spaced colonic crypts (B). High-resolution fluorescence image from area in (B) shows evenly spaced tubular structures (yellow arrow) and polarized nuclei at the crypt edges (white arrow) (C). Corresponding histopathology is shown (D).

Figure 4: White-light image dysplastic colonic mucosa is shown (A). Widefield proflavine-fluorescence image shows unevenly-spaced colonic crypts (B). The brightness of the lamina propria is variable (white boxes). High-resolution proflavine-fluorescence image from inked area indicated in (B) shows unevenly spaced tubular structures (yellow arrow) and areas of crowded nuclei (white arrow) (C). Corresponding histopathology is shown (D).

Figure 5: White-light image of severely dysplastic colonic mucosa with sub-surface adenocarcinoma is shown (A). Widefield proflavine-fluorescence image depicts irregularly shaped colonic crypts (B). High-resolution fluorescence image from area indicated in (B) shows irregularly shaped, unevenly spaced tubular structures (yellow arrow) and areas of crowded nuclei (white arrow) (C). Corresponding histopathology is shown (D).

Figure 6: White-light image of invasive adenocarcinoma is shown (A). Widefield proflavine-fluorescence image from area indicated in (A) depicts loss of regular glandular architecture (B). High-resolution fluorescence image from area indicated in (B) shows areas of dense nuclei (C). Corresponding histopathology is shown (D).

Figure 7: White-light image of an area of mildy active IBD is shown (A). Widefield proflavine-fluorescence image from area indicated in (A) depicts an irregular glandular pattern (B). High-resolution fluorescence image from area indicated in (B) shows an increase in distorted glands with cryptitis (arrow) and expanded lamina propria (C). Corresponding histopathology of active colitis is shown (D).

Figure 8: White-light image of an area of severely active IBD with ulcer is shown (A). Widefield proflavine-fluorescence image from area indicated in (A) depicts glandular irregularity (B). High-resolution fluorescence image from area indicated in (B) shows a

dense nuclear presence in the lamina propria (C). Corresponding histopathology of severe colitis is shown (D).

Table Headings:

Table 1: Image features present in proflavine-enhanced widefield and high resolution imaging of normal esophagus, Barrett's metaplasia, dysplasia, and adenocarcinoma

Table 2: Image features present in proflavine-enhanced widefield and high resolution imaging of normal colon, dysplasia, and adenocarcinoma

Table 3: Image features present in proflavine-enhanced widefield and high resolution imaging of mildly active inflammatory bowel disease (IBD) and severely active IBD.

1. Rubin DT, Rothe JA, Hetzel JT, Cohen RD, Hanauer SB. Are dysplasia and colorectal cancer endoscopically visible in patients with ulcerative colitis? Gastrointestinal Endoscopy 2007;65:998-1004.
2. Vieth M, Ell C, Gossner L, May A, Stolte M. Histological analysis of endoscopic resection specimens from 326 patients with Barrett's esophagus and early neoplasia. Endoscopy 2004;36:776-81.
3. Dekker E, van den Broek FJ, Reitsma JB, Hardwick JC, Offerhaus GJ, van Deventer SJ, Hommes DW, Fockens P. Narrow-band imaging compared with conventional colonoscopy for the detection of dysplasia in patients with longstanding ulcerative colitis. Endoscopy 2007;39:216-21.
4. van den Broek FJ, Fockens P, van Eeden S, Reitsma JB, Hardwick JC, Stokkers PC, Dekker E. Endoscopic tri-modal imaging for surveillance in ulcerative colitis: randomised comparison of high-resolution endoscopy and autofluorescence imaging for neoplasia detection; and evaluation of narrow-band imaging for classification of lesions. Gut 2008;57:1083-9.
5. Kiesslich R, Burg J, Vieth M, Gnaendiger J, Enders M, Delaney P, Polglase A, McLaren W, Janell D, Thomas S, Nafe B, Galle PR, Neurath MF. Confocal laser endoscopy for diagnosing intraepithelial neoplasias and colorectal cancer in vivo. Gastroenterology 2004;127:706-13.
6. Kiesslich R, Gossner L, Goetz M, Dahlmann A, Vieth M, Stolte M, Hoffman A, Jung M, Nafe B, Galle PR, Neurath MF. In vivo histology of Barrett's esophagus and associated neoplasia by confocal laser endomicroscopy. Clin Gastroenterol Hepatol 2006;4:979-87.
7. Pohl H, Roesch T, Vieth M, Koch M, Becker V, Khalifa AC, Meining A. Accuracy of Miniprobe Confocal Laser Microscopy for the Detection of Barrett Neoplasia. Gastrointestinal Endoscopy 2008;67:AB125-AB125.
8. Muldoon TJ, Anandasabapathy S, Maru D, Richards-Kortum R. High-resolution imaging in Barrett's esophagus: a novel, low-cost endoscopic microscope. Gastrointest Endosc 2008;68:737-44.
9. Pierce MC, Vila PM, Polydorides AD, Richards-Kortum R, Anandasabapathy S. Low-cost endomicroscopy in the esophagus and colon. Am J Gastroenterol (Accepted).
10. Kiesslich R, Neurath MF. Endoscopic detection of early lower gastrointestinal cancer. Best Pract Res Clin Gastroenterol 2005;19:941-61.
11. Roblyer D, Richards-Kortum R, Sokolov K, El-Naggar AK, Williams MD, Kurachi C, Gillenwater AM. Multispectral optical imaging device for in vivo detection of oral neoplasia. J Biomed Opt 2008;13:024019.
12. Muldoon TJ, Pierce MC, Nida DL, Williams MD, Gillenwater A, Richards-Kortum R. Subcellular-resolution molecular imaging within living tissue by fiber microendoscopy. Opt Express 2007;15:16413-23.
13. Kara MA, Peters FP, Ten Kate FJ, Van Deventer SJ, Fockens P, Bergman JJ. Endoscopic video autofluorescence imaging may improve the detection of early neoplasia in patients with Barrett's esophagus.[see comment]. Gastrointestinal Endoscopy 2005;61:679-85.
14. Kara MA, Smits ME, Rosmolen WD, Bultje AC, Ten Kate FJ, Fockens P, Tytgat GN, Bergman JJ. A randomized crossover study comparing light-induced fluorescence

endoscopy with standard videoendoscopy for the detection of early neoplasia in Barrett's esophagus. Gastrointest Endosc 2005;61:671-8.
15. Inoue H, Kazawa T, Sato Y, Satodate H, Sasajima K, Kudo SE, Shiokawa A. In vivo observation of living cancer cells in the esophagus, stomach, and colon using catheter-type contact endoscope, "Endo-Cytoscopy system". Gastrointest Endosc Clin N Am 2004;14:589-94, x-xi.
16. Sasajima K, Kudo SE, Inoue H, Takeuchi T, Kashida H, Hidaka E, Kawachi H, Sakashita M, Tanaka J, Shiokawa A. Real-time in vivo virtual histology of colorectal lesions when using the endocytoscopy system. Gastrointest Endosc 2006;63:1010-7.
17. Kiesslich R, Goetz M, Lammersdorf K, Schneider C, Burg J, Stolte M, Vieth M, Nafe B, Galle PR, Neurath MF. Chromoscopy-Guided Endomicroscopy Increases the Diagnostic Yield of Intraepithelial Neoplasia in Ulcerative Colitis. Gastroenterology 2007;132:874-882.
18. Polglase AL, McLaren WJ, Skinner SA, Kiesslich R, Neurath MF, Delaney PM. A fluorescence confocal endomicroscope for in vivo microscopy of the upper- and the lower-GI tract. Gastrointest Endosc 2005;62:686-95.
19. Janssen PA, Selwood BL, Dobson SR, Peacock D, Thiessen PN. To dye or not to dye: a randomized, clinical trial of a triple dye/alcohol regime versus dry cord care. Pediatrics 2003;111:15-20.

***Acronyms (list all acronyms used in paper with their spell-outs)**

Acronym List:

Barrett's esophagus (BE)

Esophageal adenocarcinoma (EAC)

Endoscopic mucosal resection (EMR)

Inflammatory bowel disease (IBD)

Multispectral digital microscope (MDM)

High resolution microendoscope (HRME)

Light-emitting diode (LED)

High grade dysplasia (HGD)

Gastrointestinal (GI)

Charge-coupled device (CCD)

Hematoxylin and eosin (H&E)

***Author Contributions**

Author Contributions: conception and design (N.T., S.A., R.R.K.); data collection (N.T., T.J.M, A.D.P, D.M.M., N.H.); analysis and interpretation (all authors); drafting the article (N.T.); critical revision of the article for important intellectual content (N.T., A.D.P, S.A., R.R.K.); final approval of the article (N.T., S.A., R.R.K.)

Figure 1

Click here to download high resolution image

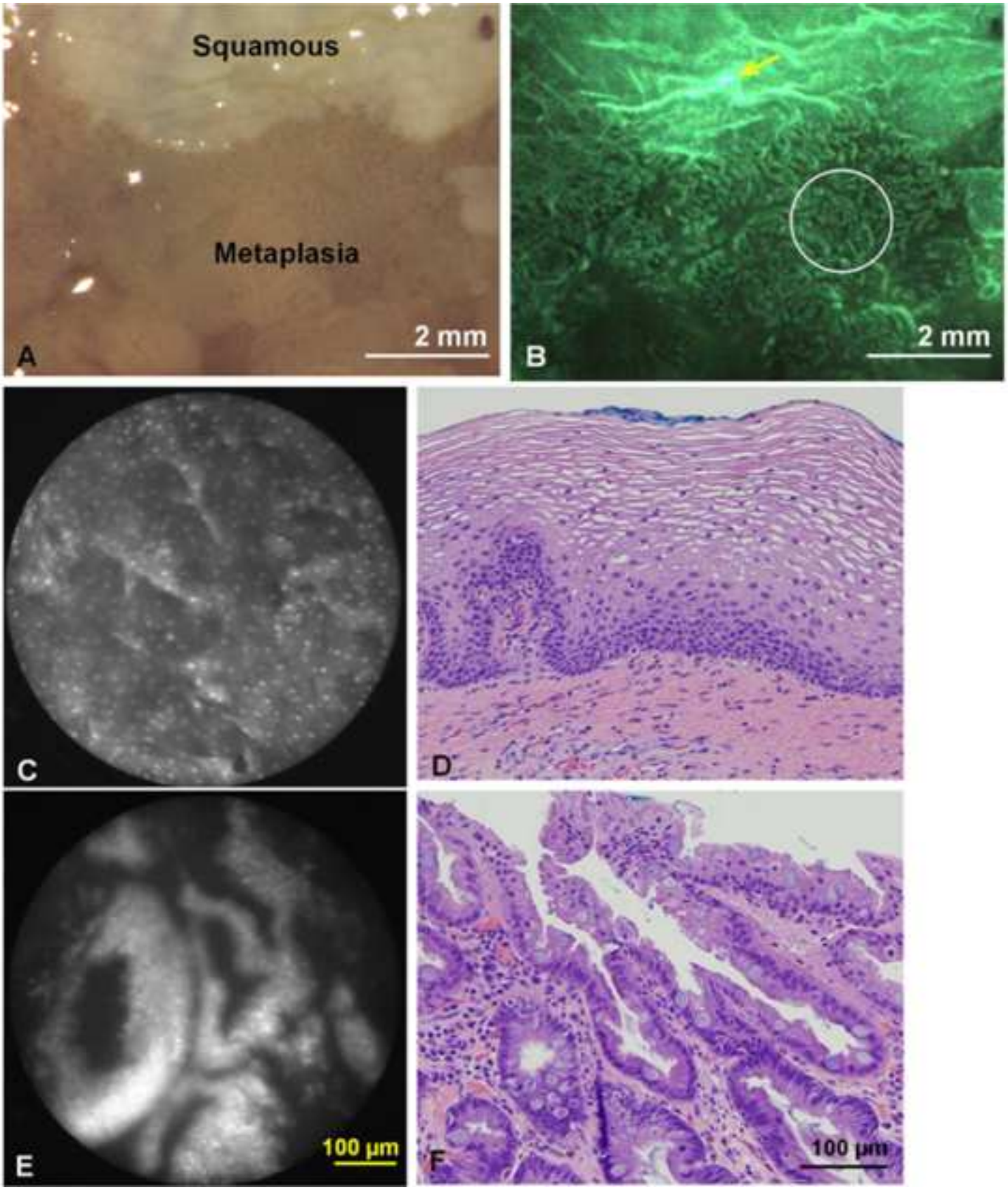

Figure 2

Click here to download high resolution image

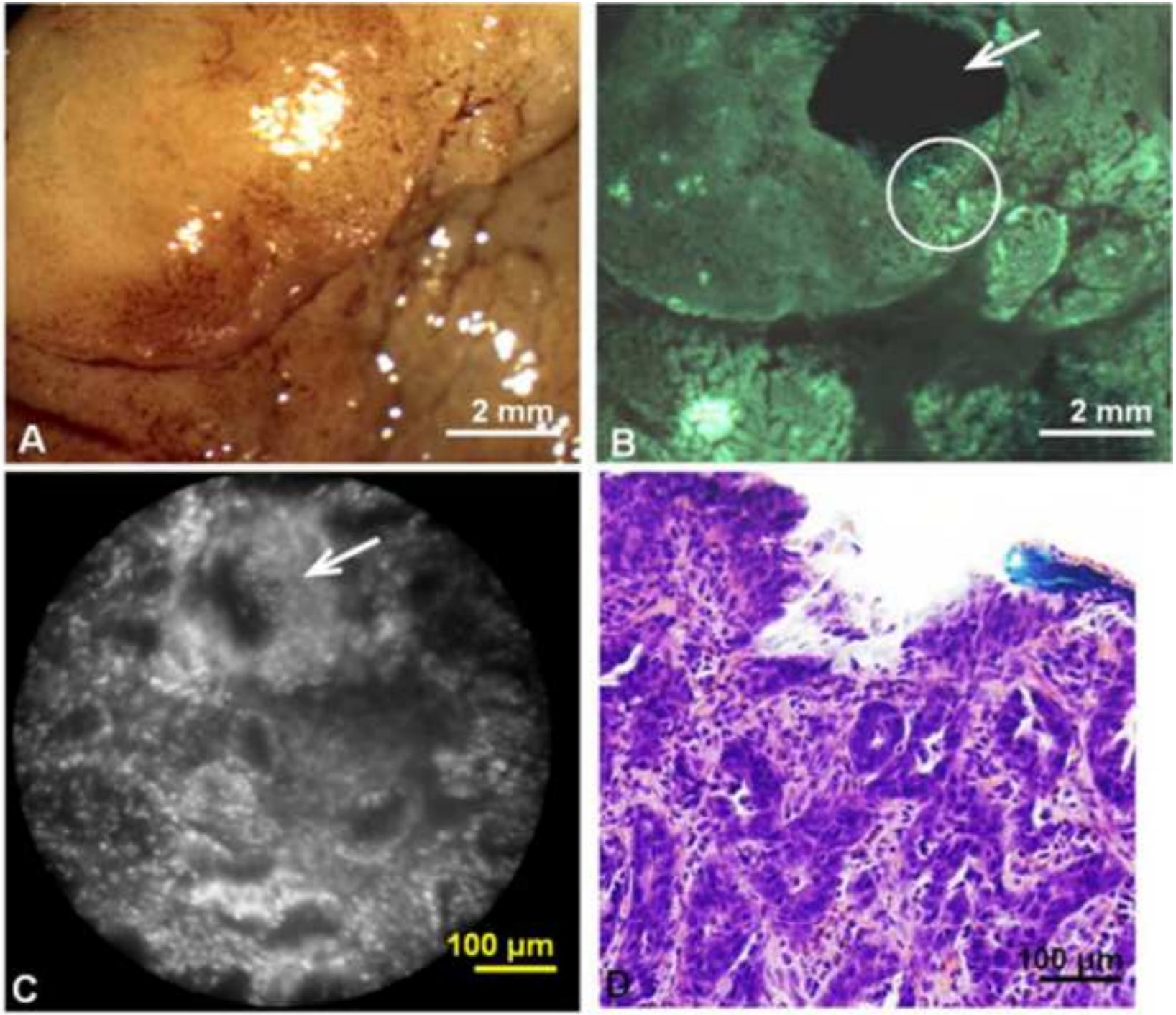

Figure 3

Click here to download high resolution image

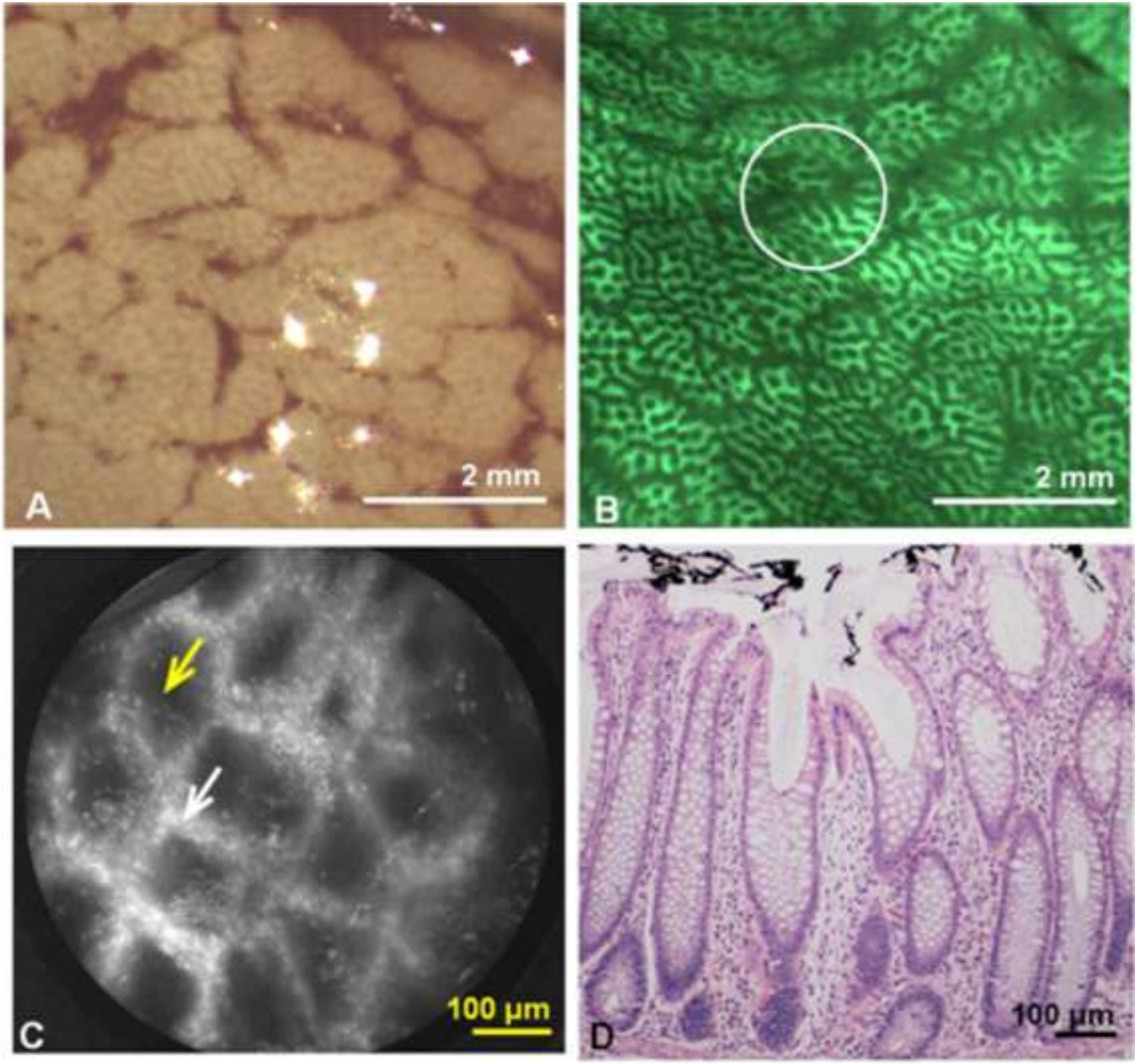

Figure 4

Click here to download high resolution image

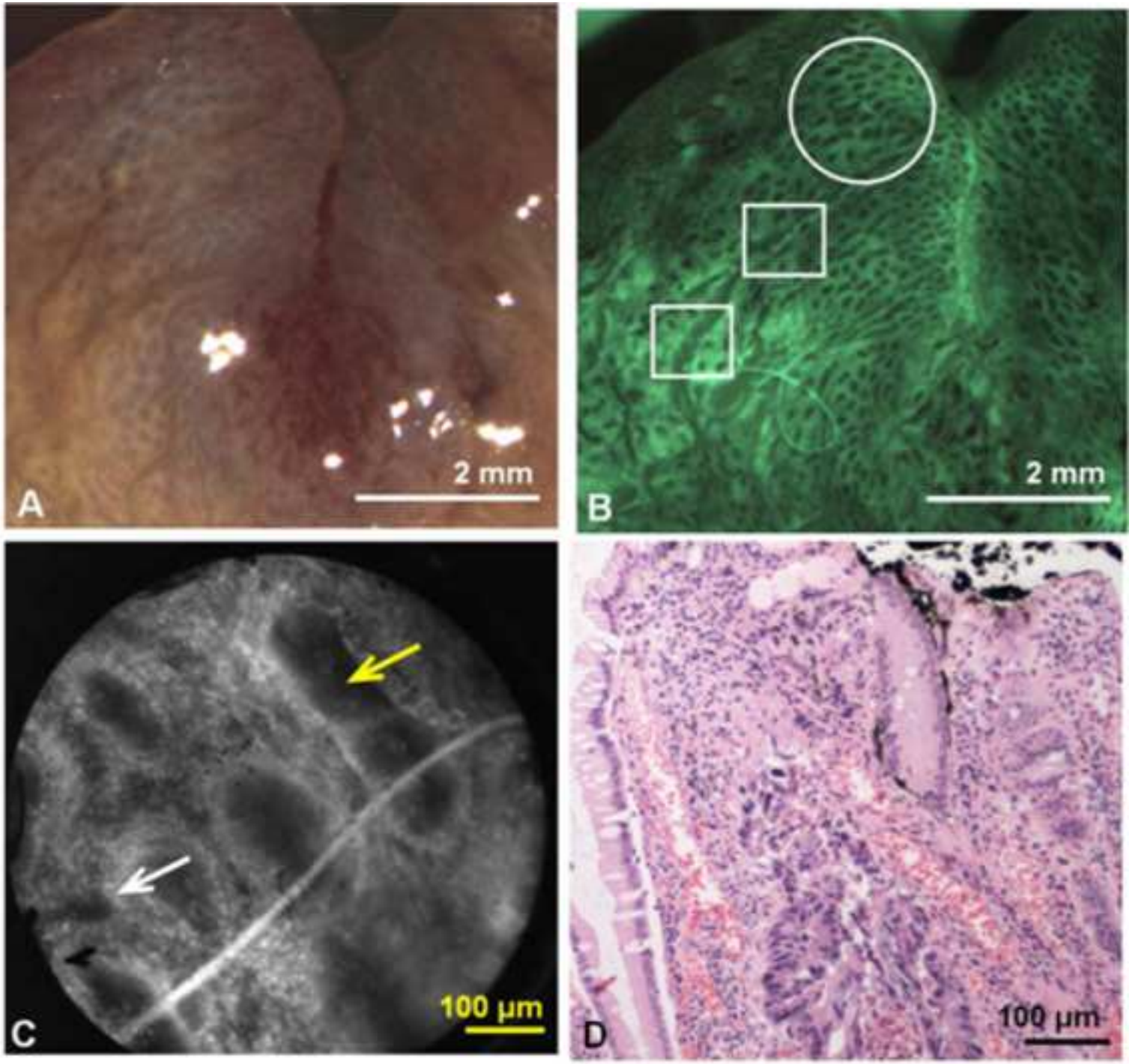

Figure 5

Click here to download high resolution image

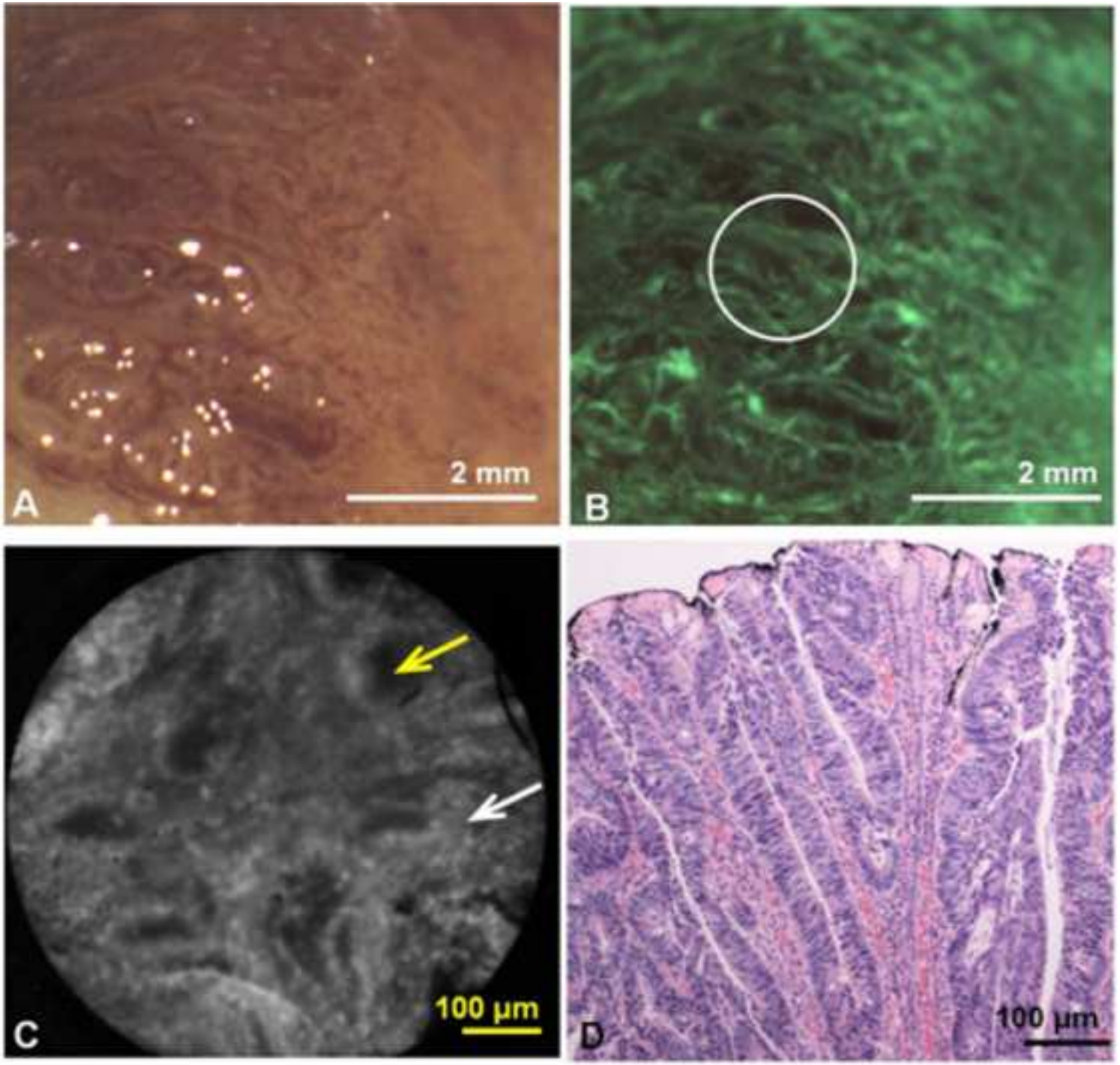

Figure 6

Click here to download high resolution image

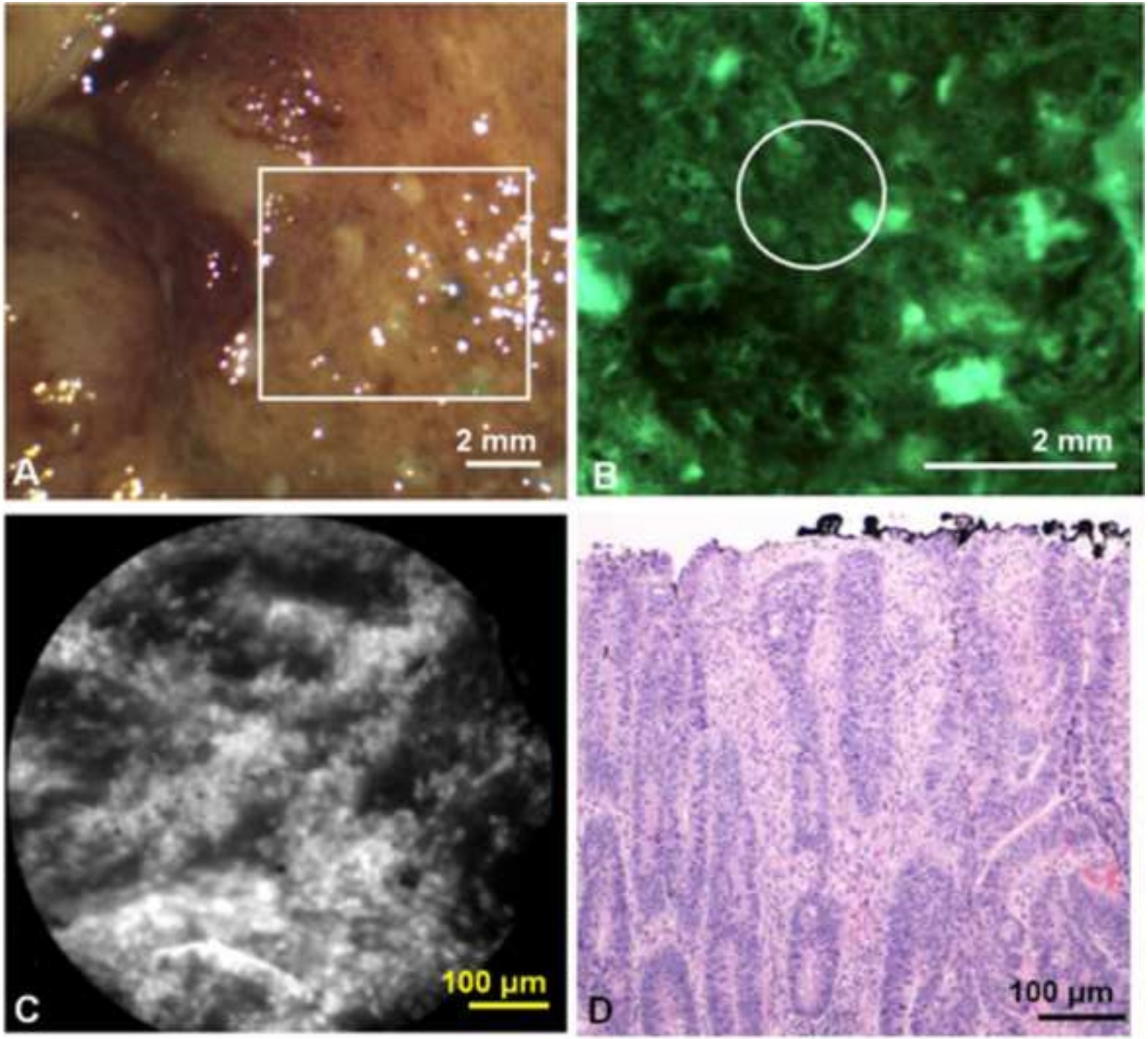

Figure 7

Click here to download high resolution image

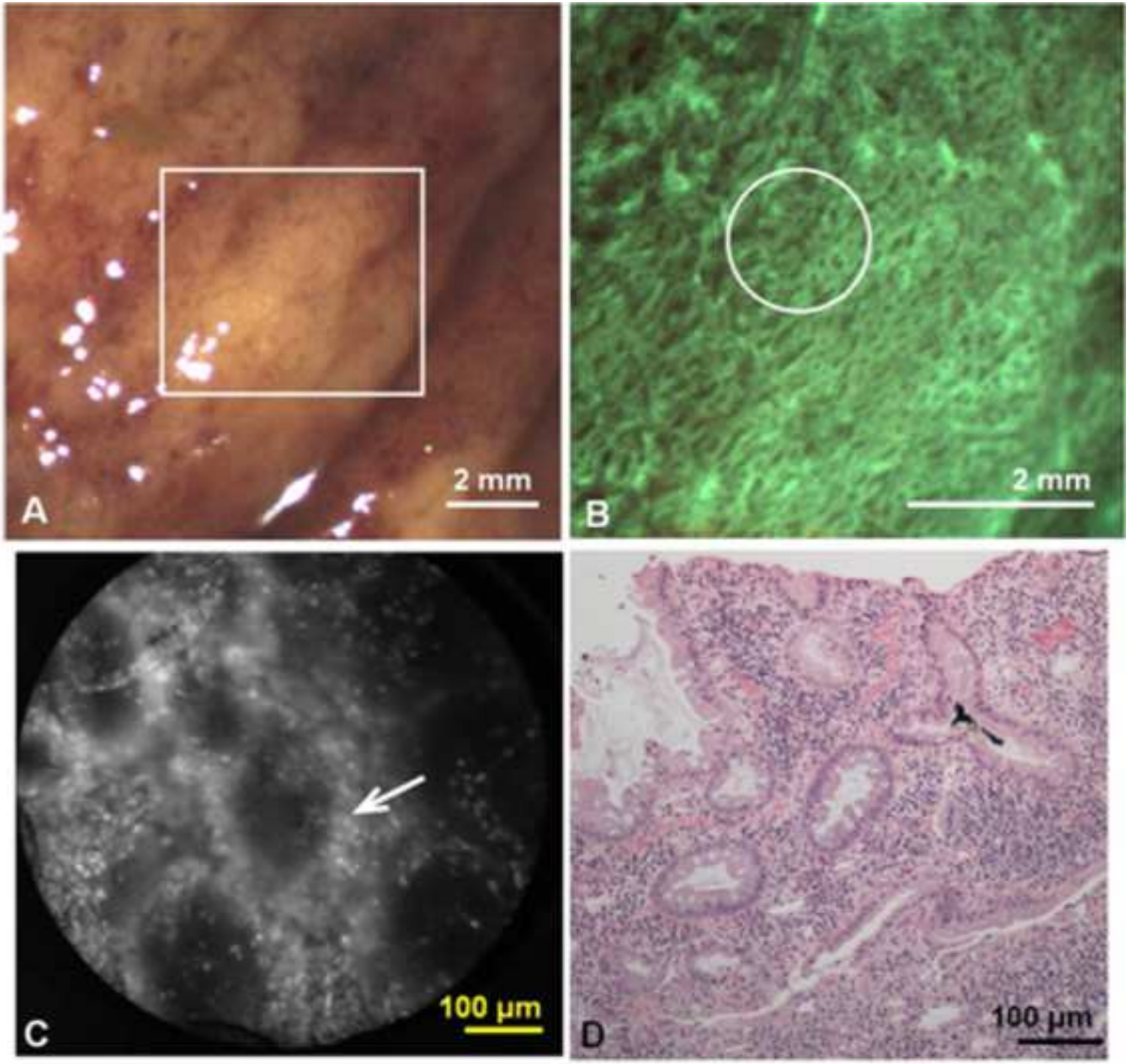

Figure 8

Click here to download high resolution image

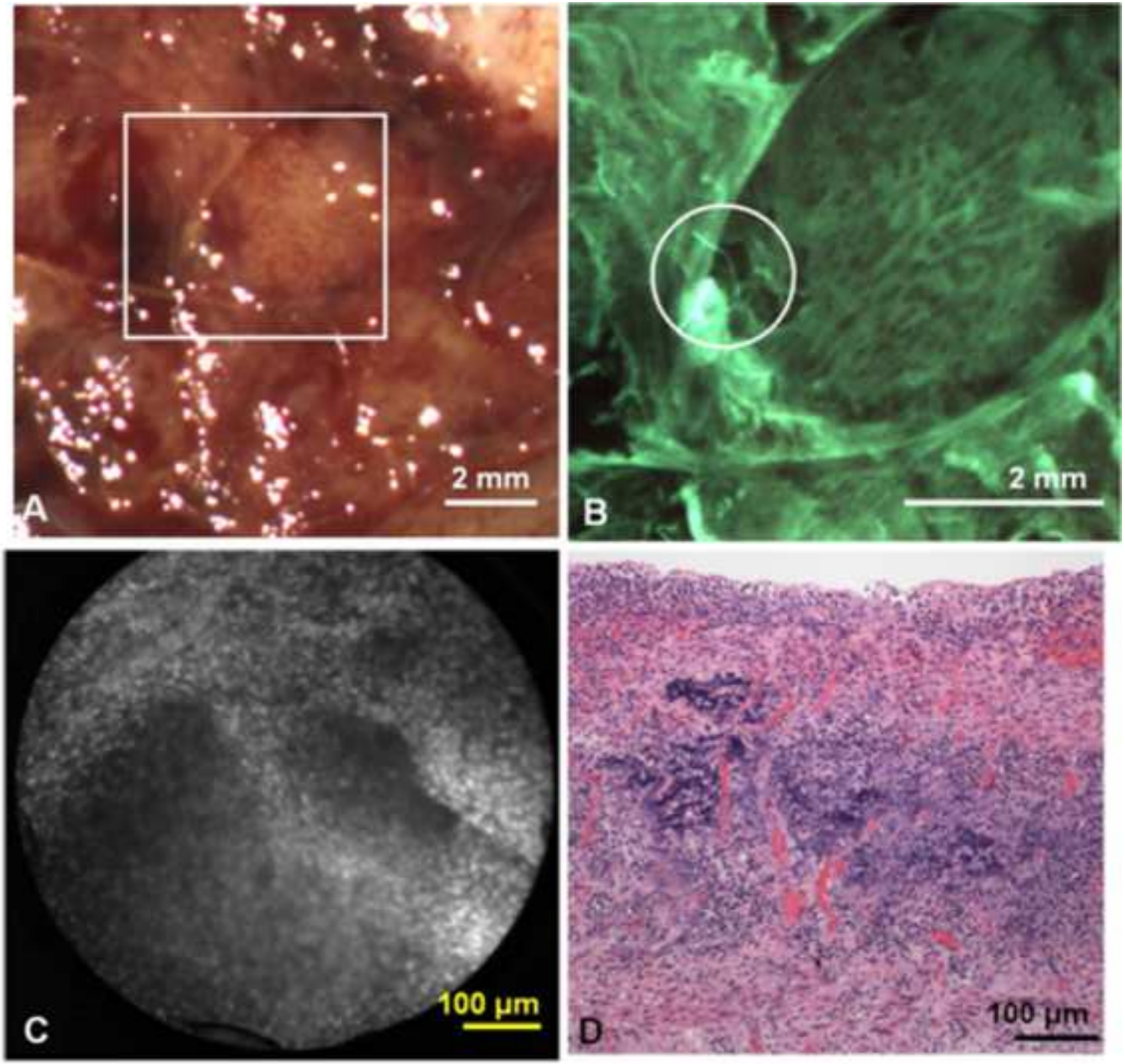

Table 1

Click here to download high resolution image

	Widefield Imaging Features		High Resolution Imaging Features	
Normal Esophageal Mucosa	No glands present	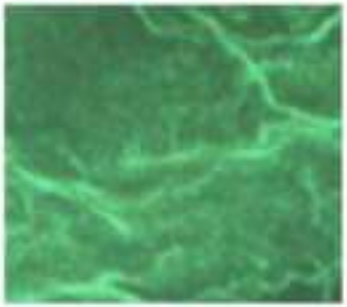	Evenly spaced, homogeneous nuclei	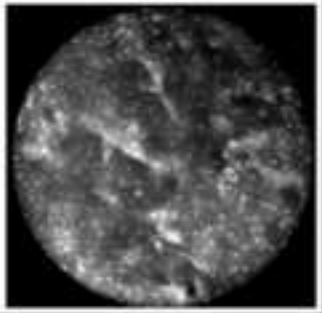
Barrett's Metaplasia	Elongated and intact glands	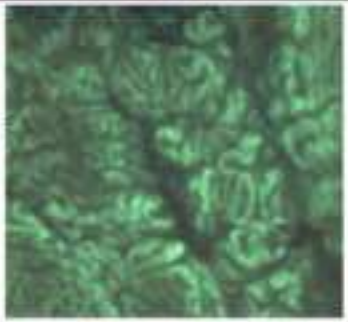	Intact glands Basal nuclei	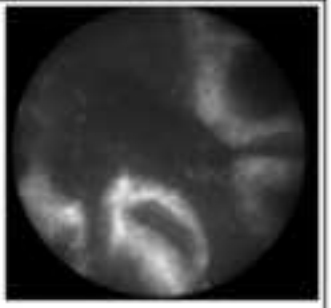
Dysplasia	Crowded and heterogeneous glands	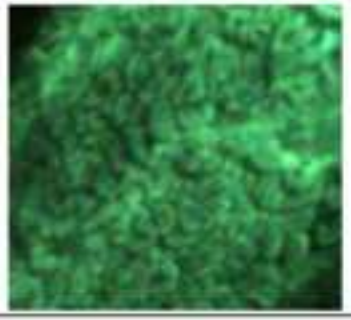	Crowded and distorted glands Nuclear crowding, enlargement and pleomorphism Loss of nuclear polarity (with high grade dysplasia)	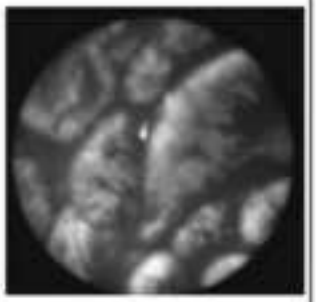
Adeno-carcinoma	Effacement of glandular architecture	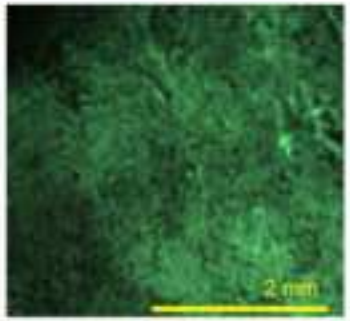	Irregular glands Invasion of lamina propria (stromal reaction)	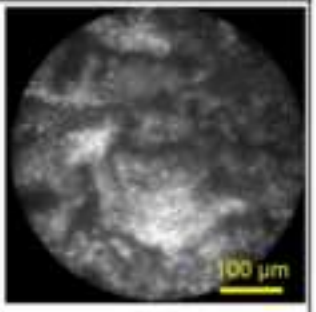

Table 2

Click here to download high resolution image

	Widefield Imaging Features		High Resolution Imaging Features	
Normal Colon Mucosa	Regular, intact tubular glandular pattern	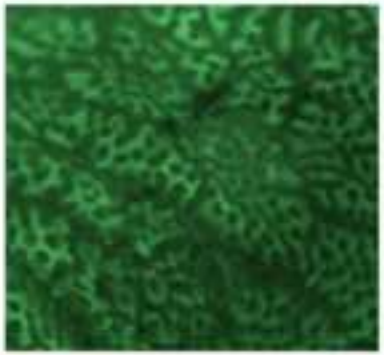	Uniform glands Regular, small, basal nuclei	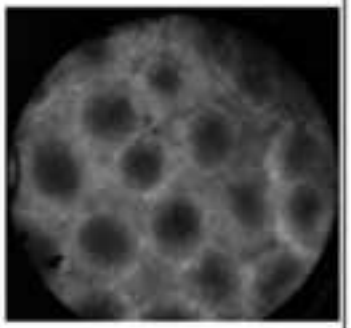
Dysplasia	Irregular, heterogeneous glands	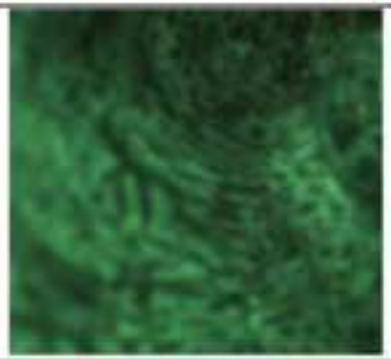	Distorted glands Nuclear crowding, enlargement and pleomorphism Loss of nuclear polarity	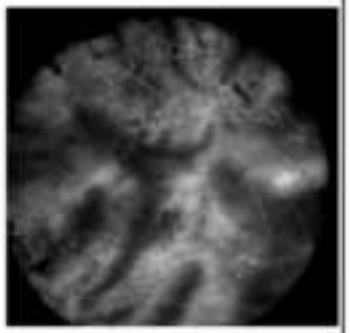
Adeno-carcinoma	Effacement of glandular architecture	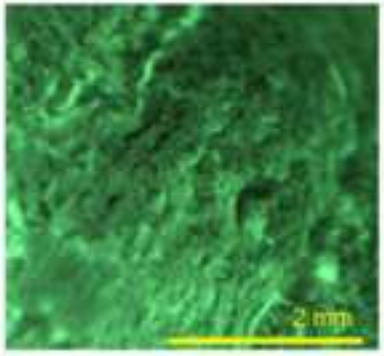	Increasingly irregular glands Invasion of lamina propria Stromal reaction	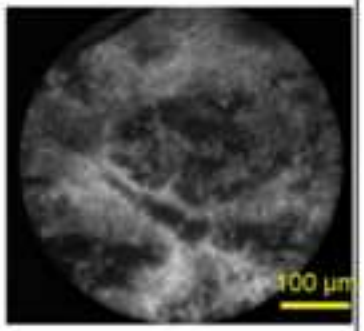

Table 3

Click here to download high resolution image

	Widefield Imaging Features		High Resolution Imaging Features	
Mildly Active IBD	Irregular glands	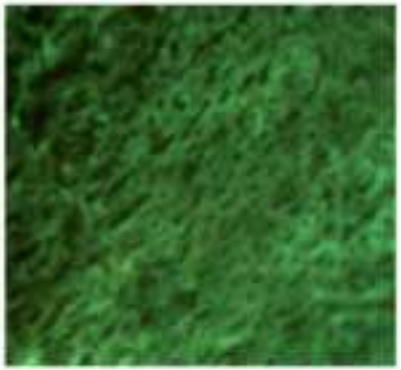	Architectural distortion and cryptitis Expanded, crowded lamina propria	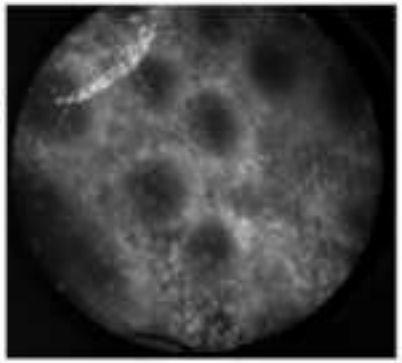
Severely Active IBD	Infrequent, heterogeneous glands	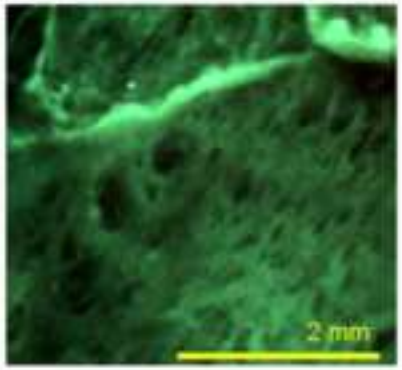	Severely atrophic glands Very expanded, crowded lamina propria